

Genomic analysis identifies risk factors in restless legs syndrome.

Fulya Akçimen¹, Ruth Chia¹, Sara Saez-Atienzar¹, Paola Ruffo^{1,2}, Memoona Rasheed¹, Jay P. Ross^{3,4}, Calwing Liao^{5,6,7}, Anindita Ray⁸, Patrick A. Dion^{4,9}, Sonja W. Scholz^{8,10}, Guy A. Rouleau^{3,4,9} & Bryan J. Traynor^{*1,10}

Author affiliations

1. Neuromuscular Diseases Research Section, National Institute on Aging, National Institutes of Health, Bethesda, MD, USA.
2. Medical Genetics Laboratory, Department of Pharmacy, Health and Nutritional Sciences, University of Calabria, Rende, Italy
3. Department of Human Genetics, McGill University, Montréal, QC, Canada
4. Montreal Neurological Institute, McGill University, Montréal, QC, Canada
5. Analytic and Translational Genetics Unit, Department of Medicine, Massachusetts General Hospital, Boston, MA, USA
6. Stanley Center for Psychiatric Research, Broad Institute of MIT and Harvard, Cambridge, MA, USA
7. Center for Genomic Medicine, Massachusetts General Hospital, Boston, MA, USA
8. Neurodegenerative Diseases Research Unit, National Institute of Neurological Disorders and Stroke, National Institutes of Health, Bethesda, MD, USA
9. Department of Neurology and Neurosurgery, McGill University, Montréal, QC, Canada
10. Department of Neurology, Johns Hopkins University Medical Center, Baltimore, MD, USA

***Corresponding Author:**

Name: Bryan J. Traynor

E-mail : bryan.traynor@nih.gov

Keywords: restless legs syndrome, *LMX1B*, *GLO1*, whole-genome sequencing, GWAS, CLSA

Title character count: 68

Word count: Abstract: 211, Main text: 3565

Tables: 4

Figures: 2

Supplementary tables: 2

Supplementary figures: 7

Conflict of interest: None.

Abstract

Restless legs syndrome (RLS) is a neurological condition that causes uncomfortable sensations in the legs and an irresistible urge to move them, typically during periods of rest. The genetic basis and pathophysiology of RLS are incompletely understood. Here, we present a whole-genome sequencing and genome-wide association meta-analysis of RLS cases ($n = 9,851$) and controls ($n = 38,957$) in three population-based biobanks (All of Us, Canadian Longitudinal Study on Aging, and CARTaGENE). Genome-wide association analysis identified nine independent risk loci, of which eight had been previously reported, and one was a novel risk locus (*LMX1B*, rs35196838, OR = 1.14, 95% CI = 1.09-1.19, p -value = 2.2×10^{-9}). A genome-wide, gene-based common variant analysis identified *GLO1* as an additional risk gene (p -value = 8.45×10^{-7}). Furthermore, a transcriptome-wide association study also identified *GLO1* and a previously unreported gene, *ELFNI*. A genetic correlation analysis revealed significant common variant overlaps between RLS and neuroticism ($r_g = 0.40$, se = 0.08, p -value = 5.4×10^{-7}), depression ($r_g = 0.35$, se = 0.06, p -value = 2.17×10^{-8}), and intelligence ($r_g = -0.20$, se = 0.06, p -value = 4.0×10^{-4}). Our study expands the understanding of the genetic architecture of RLS and highlights the contributions of common variants to this prevalent neurological disorder.

Introduction

Restless legs syndrome (RLS) is a common neurological disease characterized by an irresistible urge to move the legs¹. Affected individuals exhibit exhaustion and sleepiness, which affect daily activities, work productivity, and personal relationships^{2,3}. Studies reported that 5-15% of the European and North American populations suffer from RLS^{4,5}, leading to a substantial socio-economic burden. Familial aggregation⁶ and twin studies⁷ estimate its heritability to be approximately 70%, suggesting a major genetic predisposition to RLS. To date, linkage studies in multiplex families have implicated eight genomic regions in families with RLS⁸, and genome-wide association studies (GWASs) have identified an additional 22 genetic risk loci (23 independent variants) associated with RLS^{9,10}. Despite this, only about 12% of the heritability is explained⁹, meaning that much remains to be uncovered. Thus far, sequencing studies have been done through the targeted gene approach, and no causal variants were identified within the risk loci¹¹⁻¹³.

To address this gap and to improve our understanding of RLS's genetic architecture, we performed a large-scale genomic analysis involving 9,851 cases and 38,957 controls. We identified nine risk loci, of which one has not been previously reported, and performed functional annotations of the detected signals. We also performed pathway and genetic correlation analyses to gain insights into the underlying mechanisms and the relationship between RLS and other traits.

Methods

Samples

A total of 9,851 RLS cases and 38,957 controls of European ancestry recruited by three population-based biobanks (CARTaGENE, Canadian Longitudinal Study on Aging, and All of Us) across Canada and the United States were included in the discovery stage meta-analysis of GWAS. Survey-based identification of RLS cases in CARTaGENE and the Canadian Longitudinal Study on Aging was made through essential RLS diagnostic questions. The Personal Medical History domain was used to identify All of Us cases. Controls were selected amongst the individuals with no neurological diseases (Supplementary Table 1).

Whole genome sequencing and quality assessment

Sequencing was performed by the Genome Centers funded by the All of Us Research Program^{14,15}. All centers used the same sequencing protocols that consisted of PCR-free 150 bp, paired-end libraries sequenced on the Illumina NovaSeq 6000 platform and processed using DRAGEN v3.4.12 (Illumina) software. The GRCh38 reference genome was used for alignment¹⁶. Phenotypic data, ancestry features, and principal components were annotated using Hail through the All of Us Researcher Workbench¹⁷. Low-quality variants with a call rate of less than 0.95, multiallelic variants, and variants significantly departed from Hardy-Weinberg equilibrium in the control cohort ($P \leq 1.0 \times 10^{-10}$) were removed. Common variants in autosomal chromosomes with a minor allele frequency of higher than 0.005 were included in the association test. Sex concordance was part of the All of Us upstream genomic data quality control process, and all samples within the released genomic data have passed the sex

concordance check. Ancestry annotation and relatedness were inferred by the PC-relate method in Hail. Duplicate samples and one of the related participant pairs were excluded¹⁷.

Genotyping and imputation

Genotyping data were generated using the Illumina Global Diversity Array for All of Us (1,825,277 markers/GDA-8 v1.0/12,114 participants), Affymetrix protocol for Canadian Longitudinal Study on Aging (794,409 markers/ Axiom 2.0 /29,970 participants), and Illumina Infinium Global Screening Array technology for CARTaGENE (700,078 markers/GSAMD-24v1-0_20011747_A1/2,228 participants). Further cohort and quality control details for the Canadian Longitudinal Study on Aging and CARTaGENE data sets are described in Awadella et al.¹⁸ and Forgetta et al.¹⁹. The same quality assessment, filtering, and imputation protocols were applied for all three genotyping cohorts and are summarized in Figure 1. Samples were excluded if missingness was higher than 5% or the reported and genotypic sex was discordant. KING²⁰ was used to determine pairwise kinship and ancestry estimation²¹. Unrelated participants with European ancestry were kept for subsequent analyses. Quality assessment for missingness, sex concordance, Hardy-Weinberg equilibrium, and minor allele frequency was conducted using PLINK 2.0²². Multiallelic and non-autosomal variants were removed. Variants with a genotyping call rate of less than 99%, a minor allele frequency of less than 0.01, showing nonrandom missingness between cases and controls ($P \leq 1.0 \times 10^{-4}$), and variants that significantly departed from Hardy-Weinberg equilibrium in the control cohort ($P \leq 1.0 \times 10^{-10}$) were excluded.

Imputation was carried out using Minimac4 phasing with Eagle v2.4 Trans-Omics for Precision Medicine (TopMed) imputation reference panel (hg38) on TopMed Imputation Server²³⁻²⁵. The Canadian Longitudinal Study on Aging cohort was previously imputed via the same pipeline using the

TopMed imputation reference panel¹⁹. After the imputation, variants with a minor allele frequency of less than 0.5% and an imputation quality score of less than 0.5 were excluded prior to the association test.

Single variant association test and meta-analysis

We generated principal components in PLINK (version 2.0)²². We used the step function in the R MASS package to determine the optimum combination of covariates (age, sex, and principal components) to be included in the association tests²⁶ (Supplementary Table 3). We performed a logistic regression analysis in PLINK v.2.0²² separately in all datasets and meta-analyzed the results using an inverse-variance-weighted meta-analysis in METAL²⁷. We included only the variants that were present in all datasets in the final meta-analysis and set the Bonferroni threshold for genome-wide significance as 5.0×10^{-8} . For follow-up replication of the significant associations in this study, we used the summary statistics of the previous GWAS results by Didriksen et al., which included 10,257 cases and 470,725 controls¹⁰. The heritability explained by variants tested in our meta-analysis was estimated via LD Score Regression v.1.0.1 using the 1000 Genomes Project cohort for linkage disequilibrium and allele frequencies. We used MungeSumstats to perform standardization of association statistics²⁸. We conducted a conditional analysis in PLINK v.2.0 to identify potential secondary signals in the *LMX1B* and *BTBD9* loci that may have been missed in the initial GWAS. The conditional analysis was performed by including the index variant at each locus to the covariates of the logistic regression analyses.

Genome-wide, gene-based association analyses

Gene-based associations with RLS were estimated with SNP2GENE function in FUMA (v.1.5.1)²⁹ using the summary statistics from the RLS meta-analysis (n = 9,851 cases and 38,957 controls). First, we annotated genes that contain RLS-associated variants. For gene annotations, we included all variants that are in linkage disequilibrium ($r^2 > 0.6$) with the genome-wide significant signals ($P < 5 \times 10^{-8}$). We used UK Biobank European population as a reference panel to define the linkage disequilibrium between variants. Second, we performed a gene-burden analysis using MAGMA (v.1.08)³⁰ implemented in FUMA²⁹.

For the rare variant burden test, we utilized WGS data of 1,977 cases and 10,137 controls in the All of Us biobank. We annotated potentially disruptive variants using the VEP³¹ and its plugin, Loss-Of-Function Transcript Effect Estimator (LOFTEE)³². We performed genome-wide, gene-based SKAT-O analysis using RVTEST (v.2.1.0). We incorporated age, sex, PC2, PC3, PC7, and PC10 as covariates determined by the R MASS package.

Transcriptome-wide association and fine mapping

For transcriptomic imputation, we applied FUSION³³ (lasso, susie, top1) and S-PrediXcan³⁴ (elastic net, mashr). We tested the differential expression of the available gene models in 13 brain tissue panels imputed in GTEx version 8 of European samples (Table 3). To account for the large number of hypotheses tested, we used a Bonferroni correction p-value of 2.10×10^{-6} for FUSION ($\alpha = 0.05/23,770$ genes tested) and a p-value of 3.06×10^{-6} for S-PrediXcan ($\alpha = 0.05/16,355$ genes tested). We conducted a fine mapping approach using FOCUS (v.0.802)³⁵. We used our summary statistics, a multiple-eQTL database containing FUSION GTEx version 8 weights, and the 1000 Genomes Project dataset as reference LD. FOCUS assigned a posterior probability of causality for each

gene. Finally, the genes in the 90%-credible set with a higher posterior probability were prioritized as putatively causal.

Regulome-wide association study

RWAS was conducted using the linear model implemented in MAGMA (v.1.10)³⁶. Enhancer annotations for eight brain regions (hippocampus, dorsolateral prefrontal cortex, angular gyrus, anterior caudate, cingulate gyrus, inferior temporal lobe, substantial migration, and germinal matrix) were downloaded from the psychENCODE consortium (<http://resource.psychencode.org/>) and updated in GRCh38 assembly.

Gene-set enrichment and pathway analysis

A gene-set enrichment analysis approach was conducted using public datasets containing GO (<http://geneontology.org>) and Reactome (<https://reactome.org>) pathways in EnrichR^{37,38}.

Genetic correlation

We assessed the genetic correlation between RLS and the following neurological or neuropsychiatric traits of interest with publicly available summary statistics of meta-analysis: Alzheimer's disease³⁹, attention deficit hyperactivity disorder⁴⁰, depression⁴¹, insomnia⁴², intelligence⁴³, neuroticism⁴⁴, and serum iron and ferritin levels⁴⁵. We used LD score regression⁴⁶ with recommended LD scores from the 1000 Genomes Project. A Bonferroni correction p-value of 0.00625 ($\alpha = 0.05/8$ traits testes) was defined for the significance threshold.

Results

Genome-wide inferences

We performed a meta-analysis of GWAS in a total of 9,851 RLS cases and 38,957 controls of European ancestry. These samples included the ‘All of Us’ whole-genome sequencing cohort (1,977 cases and 10,137 controls), the ‘All of Us’ genotyping cohort (1,973 cases and 11,523 controls), the Canadian Longitudinal Study on Aging (4,980 cases and 15,990 controls)⁴⁷, and CARTaGENE (921 cases and 1,307 controls) (Figure 1, Supplementary Table 1). After imputation, quality assessment, and filtering, we performed a GWAS of RLS based on 7,510,495 variants. The estimated sample-size-adjusted genome-wide inflation factor ($\lambda_{1,000}$) was 1.0036, indicating minimum residual population structure and confounding.

We identified nine genetic loci that achieved genome-wide significance. Eight of these loci have been previously reported, and one was novel (Table 1). Annotation of the significant variants is provided in Supplementary Table 2. The index variant at this novel RLS-locus was close to the gene *LMX1B* on chromosome 9q33.3 (rs35196838, p -value = 2.2×10^{-9} , OR = 1.14, 95% CI = 1.09–1.19). A conditional analysis did not reveal a secondary signal at this locus (see Supplementary Figure 1 for the regional association and conditional association plots). We replicated the *LMX1B* (rs35196838) variant in an independent cohort of 10,257 cases and 470,725 controls (rs35196838, p -value = 2.6×10^{-5} , OR = 1.10, 95% CI = 1.05–1.14) (Table 1).

Variants in eight known RLS loci exceeded genome-wide significance in our discovery meta-analysis. Nine out of seventeen previously reported risk variants were replicated at Bonferroni significance (p -

value $\leq 0.05/17$ variants = 2.94×10^{-3}) (Supplementary Table 4). The variant-based heritability was estimated to be 10.17%, whereas the nine significant loci explained 2.16% of the phenotype (21% of the total SNP heritability).

The *TOX3* locus (16q12.1) identified in our RLS meta-analysis is also significantly associated with Parkinson's disease risk (rs3104783, p -value = 1.29×10^{-12} , OR = 1.07, 95% CI = 1.05–1.09)⁴⁸.

However, the direction of the association of this variant in RLS and Parkinson's disease is different⁴⁹.

To further explore the involvement of *TOX3* variants in these two diseases, we created a beta-beta plot and identified a negative correlation coefficient of -0.95 and a Pearson correlation R^2 of 0.91 (Supplementary Figure 2).

Gene-burden analysis

To identify genes with variants driving the risk of RLS, we performed a gene-based association analysis using the results of the GWAS meta-analysis using MAGMA (v.1.08)³⁰, as implemented in FUMA²⁹.

We found six significant gene-level associations that achieved genome-wide significance ($< 0.05/18,623$ protein-coding genes tested = 2.69×10^{-6}). The strongest of these signals was *BTBD9* (p -value = 3.79×10^{-17}), followed by *TOX3* (p -value = 5.77×10^{-13}), both of which are well-established RLS risk loci^{9,50,51}. In addition to these GWAS risk genes, we showed that *GLO1*, near the *BTBD9* locus, was significantly associated with RLS (p -value = 8.45×10^{-7}) (Figure 2b). A conditional analysis showed only one signal near *BTBD9* and *GLO1* (see Supplementary Figure 1c for the regional association plot and Supplementary Figure 1d for the conditional association analysis).

We also employed a rare variant burden test to investigate the contribution of rare variants in RLS. Following quality control of sequencing data and annotations, 21,335 genes were tested for rare variant burden in 1,977 cases and 10,137 controls. We subset the rare variants ($MAF < 0.005$) into high-confidence (such as stop gain or loss, frameshifts, and splice donor or acceptors) and moderate groups (such as missense, inframe insertions, or deletions) based on their calculated variant consequences by VEP³¹. Considering the possible regulatory role of intronic variants, we also conducted the burden test to a group of all rare intragenic variants regardless of their annotation. Our gene-based burden tests did not identify enrichment for rare intragenic single nucleotide variants.

Transcriptome-wide association study identifies new genes associated with RLS.

We sought to integrate expression quantitative trait locus (eQTL) analyses using publicly available transcriptomic data with summary-level GWAS results. To do so, we used two transcriptomic imputation approaches, FUSION³³ and S-PrediXcan³⁴, and tested the differential expression of these gene models in 13 brain tissues (Table 3). We identified 21 associations for seven genes at the transcriptome-wide significant level (Figure 2c), of which four were not identified in the previous transcriptome-wide association study (TWAS) for RLS: *GLO1* (6p21), *ELFNI* (7p22.3), *UBASH3B* (11q24.1), and *CAPNS1* (19q13)⁵². Consistent with previous findings, the expression of three known RLS genes, *MEIS1*, *SKOR1*, and *MAP2K5*, were also associated with RLS⁵²⁻⁵⁴. A fine-mapping analysis using the ‘Fine mapping Of CaUsal gene Sets’ (FOCUS) software (v.0.802)³⁵ prioritized *SKOR1*, *PTPRD-AS1*, *PRMT6*, *STEAP2*, and *GTPBP10* as putative candidate genes for RLS with posterior probabilities of 0.69, 0.13, 0.06, 0.06, and 0.02, respectively (Supplementary Table 6).

Regulatory regions are associated with RLS.

We performed a regulome-wide association study (RWAS) using MAGMA³⁶ to identify tissue-specific enhancer and promoter regions associated with RLS. After multiple test corrections for the number of regulatory regions tested in each tissue, we identified significant enrichments of the regulatory regions in *MEIS1*, *BTBD9*, *GLO1*, *PTPRD*, *MAP2K5*, *CASC16*, and *TOX3* (See Table 4 for the most significant enrichment for each gene and Supplementary Table 6 for all associations).

Gene-set enrichment and pathway analysis

We conducted a gene-set enrichment analysis using Reactome (<https://reactome.org>) and Gene Ontology (GO; <http://geneontology.org>) to identify biological pathways associated with the annotated genes. We identified several relevant gene sets including pathways related to neuron differentiation (GO:0030182, *PTPRD*; *SALL1*; *IRX5*; *IRX6*; *PBX3*; and *LMX1B*), generation of neurons (GO:0048699, *PTPRD*; *IRX5*; *IRX6*; *LMX1B*; *MDGA1*) and regulation of myeloid cell differentiation (GO:0045637, *PRMT6*; *MEIS1*) (Supplementary Table 7).

Genetic correlation

We calculated the genome-wide genetic correlation between pairs of traits using the LD score regression method. After correcting for multiple testing ($0.05/7 = 0.007$), we identified a significant genetic correlation between RLS and neuroticism⁴⁴ ($r_g = 0.40$, $se = 0.08$, $p\text{-value} = 5.4 \times 10^{-7}$), depression⁴¹ ($r_g = 0.35$, $se = 0.06$, $p\text{-value} = 2.17 \times 10^{-8}$), and intelligence⁴³ ($r_g = -0.20$, $se = 0.06$, $p\text{-value} = 4.0 \times 10^{-4}$) (Table 4).

Discussion

In the current study, we performed a large GWAS using population-based RLS case-control cohorts that had not been previously studied. We identified and replicated a novel genome-wide significant association in the chromosome 9q33.3 region near *LMX1B*. We also replicated the association of eight known RLS loci at a genome-wide significant level consistent with prior studies^{9,10}.

LMX1B encodes a homeodomain transcription factor involved in the early specification of midbrain dopaminergic neurons and plays a role in neuronal homeostasis in the adult brain^{55,56}. Interestingly, *Lmx1b* has also been shown to have a regulatory role in the autophagic lysosomal degradation pathway and intracellular transport functions, where its dysfunction is associated with Parkinson's disease pathogenesis⁵⁷. The altered dopaminergic system is one of the pathological elements in RLS as well, and the implication of *LMX1B* in RLS suggests an overlap between RLS and Parkinson's disease in terms of their pathogenesis. Moreover, *TOX3* locus (16q12.1), one of the first identified risk factors for RLS, was also shown to be significantly associated with Parkinson's disease⁴⁸. Together with the previous reports, our findings corroborate the involvement of common molecular mechanisms, and further investigations would help unravel the precise pathways through these common genetic risk factors in RLS and Parkinson's disease.

In addition to a variant-based analysis, we explored the collective effects of common genetic markers within genes as well as integrated transcriptomic data to identify differentially expressed genes in RLS. Our gene-based approaches identified significant associations for several genes, including well-established RLS risk loci such as *MEIS1*, *SKOR1*, *MAP2K5*, and *TOX3*. Furthermore, previous

identification of MEIS1 protein binding sites within *SKOR1* promoter regions and the regulatory effect of MEIS1 on *SKOR1* expression has prompted our investigation into other regulatory elements that may be associated with the risk of RLS⁵⁴. Interestingly, we identified significant associations of enhancers within the known RLS risk genes, including *MEIS1*, *BTBD9*, *GLO1*, *PTPRD*, *MAP2K5*, *CASC16*, and *TOX3*. These results highlighted the potential implication of non-coding regulatory regions in RLS.

Both TWAS and MAGMA analyses identified *GLO1*, located near the *BTBD9* locus, which was previously suggested as an RLS risk gene but had not been replicated yet^{11,58,59}. Notably, our TWAS detected a significant association of *GLO1* in 13 gene models in 9 tissues. *GLO1* encodes a major catabolic enzyme, glyoxalase-1, which is involved in the detoxification of methylglyoxal⁶⁰; thus, its inhibition results in the accumulation of reactive carbonyl compounds^{61,62}. Considering the implication of methylglyoxal in Parkinson's disease-like phenotypes⁶³ as well as its role in Alzheimer's disease pathogenesis⁶⁴, our results pinpoint methylglyoxal as a potential therapeutic target for RLS.

Our TWAS showed that increased expression of *ELFNI* (in cis with 7p22.3 locus) is associated with RLS. *ELFNI* has relevant implications in the brain^{65,66} and is associated with several neuropsychiatric and neurodevelopmental disorders, including intellectual disability, attention deficit hyperactivity disorder, and epilepsy⁶⁶⁻⁶⁸. Elfn1 protein has been shown to play a role in the modulation of synaptic transmission through its trans interaction with the metabotropic glutamate receptors⁶⁹, which serve as therapeutic targets for several neurological diseases, including Alzheimer's disease, epilepsy, and Parkinson's disease⁷⁰⁻⁷². Therefore, *ELFNI* may be a promising gene target for functional follow-up in RLS. TWAS also identified two previously unreported genes that are not in cis with any of the GWAS risk loci identified, *UBASH3B* and *CAPSNI*. Although trans-eQTLs could be relevant for many complex

diseases, their effect is weaker, and this low statistical power yields low replication rates^{73,74}. Therefore, association of these genes should be interpreted with caution. Overall, this integration of transcriptomic information provides additional evidence for the involvement of the associated genes in RLS and expands our understanding of the molecular mechanisms underlying the disorder.

Our study has limitations. The limited availability of non-European samples hindered our ability to carry out comprehensive analyses involving multiple ancestral groups. In addition, cases and controls were selected based on self-report, which may result in diagnostic errors. Nevertheless, the replication of previous findings and overall consistency among the three cohorts used in this study suggested that population-based biobanks are able to capture the pertinent genetic patterns.

Data availability

The GWAS summary statistics generated in this study have been deposited NHGRI-EBI GWAS Catalog at <https://www.ebi.ac.uk/gwas/> (accession IDs GCSTXXXXX). Data are available from the Canadian Longitudinal Study on Aging (www.clsa-elcv.ca) for researchers who meet the criteria for access to de-identified CLSA data.

Author contributions

FA conceived the study, analyzed the data, and wrote the first draft. PR performed the regulome-wide association study. MR assisted with the annotation for the rare-variant association test. RC, SS, JPR, CL, and AR contributed intellectually to data analysis and manuscript editing. PT, BJT, GAR, and SWS conceptualized and supervised the study. All authors critically reviewed and edited the article.

Acknowledgments

This research was undertaken in part by the Fonds de Recherche du Québec–Santé. J.P.R. has received a Canadian Institutes of Health Research Frederick Banting & Charles Best Canada Graduate Scholarship (FRN 159279). C. L. has received a CIHR Banting Fellowship. G.A.R. holds a Canada Research Chair in Genetics of the Nervous System and the Wilder Penfield Chair in Neurosciences. This work was supported in part by the NIH Intramural Research Program, the US National Institute on Aging (NIA) grant Z01-AG000949-02 and the US National Institute of Neurological Disorders and Stroke (NINDS) grants NS03130 and ZIANS003154. This study has used the high-performance computational capabilities of the Biowulf Linux cluster at the National Institutes of Health, Bethesda, MD, USA (<https://biowulf.nih.gov>). The All of Us Research Program is supported by the National Institutes of Health, Office of the Director: Regional Medical Centers: 1 OT2 OD026549; 1 OT2 OD026554; 1 OT2 OD026557; 1 OT2 OD026556; 1 OT2 OD026550; 1 OT2 OD 026552; 1 OT2 OD026553; 1 OT2 OD026548; 1 OT2 OD026551; 1 OT2 OD026555; IAA #: AOD 16037; Federally Qualified Health Centers: HHSN 263201600085U; Data and Research Center: 5 U2C OD023196; Biobank: 1 U24 OD023121; The Participant Center: U24 OD023176; Participant Technology Systems Center: 1 U24 OD023163; Communications and Engagement: 3 OT2 OD023205; 3 OT2 OD023206; and Community Partners: 1 OT2 OD025277; 3 OT2 OD025315; 1 OT2 OD025337; 1 OT2 OD025276. In addition, the All of Us Research Program would not be possible without the partnership of its participants. This research was made possible using the data/biospecimens collected by the Canadian Longitudinal Study on Aging (CLSA). Funding for the Canadian Longitudinal Study on Aging (CLSA) is provided by the Government of Canada through the Canadian Institutes of Health Research (CIHR) under grant reference: LSA 94473 and the Canada Foundation for Innovation, as well as the following provinces, Newfoundland, Nova Scotia, Quebec, Ontario, Manitoba, Alberta, and British Columbia. This research

has been conducted using the CLSA dataset [Identification of genetic loci associated with restless legs syndrome in the Canadian population, CLSA Comprehensive Follow-up 1 dataset version 3.1, and Comprehensive Baseline dataset version 6.1 and Genome-wide Genetic Data - Version 3.0, under Application Number 2104033]. The CLSA is led by Drs. Parminder Raina, Christina Wolfson and Susan Kirkland. We thank the CARTaGENE participants and team for data collection and assistance. This research has been conducted using data from CARTaGENE under project number 297405 (<https://cartagene.qc.ca/en>).

References

1. Allen RP, Picchiatti D, Hening WA, et al. Restless legs syndrome: diagnostic criteria, special considerations, and epidemiology. A report from the restless legs syndrome diagnosis and epidemiology workshop at the National Institutes of Health. *Sleep Med.* Mar 2003;4(2):101-19. doi:10.1016/s1389-9457(03)00010-8
2. Allen RP, Walters AS, Montplaisir J, et al. Restless legs syndrome prevalence and impact: REST general population study. *Arch Intern Med.* Jun 13 2005;165(11):1286-92. doi:10.1001/archinte.165.11.1286
3. Fehnel S, Zografos L, Curtice T, Shah H, McLeod L. The burden of restless legs syndrome: an assessment of work productivity, sleep, psychological distress, and health status among diagnosed and undiagnosed individuals in an internet-based panel. *Patient.* Jul 1 2008;1(3):201-10. doi:10.2165/1312067-200801030-00007
4. Ohayon MM, O'Hara R, Vitiello MV. Epidemiology of restless legs syndrome: a synthesis of the literature. *Sleep Med Rev.* Aug 2012;16(4):283-95. doi:10.1016/j.smrv.2011.05.002
5. Akcimen F, Ross JP, Sarayloo F, et al. Genetic and epidemiological characterization of restless legs syndrome in Quebec. *Sleep.* Apr 15 2020;43(4)doi:10.1093/sleep/zsz265
6. Xiong L, Montplaisir J, Desautels A, et al. Family study of restless legs syndrome in Quebec, Canada: clinical characterization of 671 familial cases. *Arch Neurol.* May 2010;67(5):617-22. doi:10.1001/archneurol.2010.67
7. Xiong L, Jang K, Montplaisir J, et al. Canadian restless legs syndrome twin study. *Neurology.* May 8 2007;68(19):1631-3. doi:10.1212/01.wnl.0000261016.90374.fd
8. Jimenez-Jimenez FJ, Alonso-Navarro H, Garcia-Martin E, Agundez JAG. Genetics of restless legs syndrome: An update. *Sleep Medicine Reviews.* Jun 2018;39:108-121. doi:10.1016/j.smrv.2017.08.002
9. Schormair B, Zhao C, Bell S, et al. Identification of novel risk loci for restless legs syndrome in genome-wide association studies in individuals of European ancestry: a meta-analysis. *Lancet Neurol.* Nov 2017;16(11):898-907. doi:10.1016/S1474-4422(17)30327-7
10. Didriksen M, Nawaz MS, Dowsett J, et al. Large genome-wide association study identifies three novel risk variants for restless legs syndrome. *Commun Biol.* Nov 25 2020;3(1):703. doi:10.1038/s42003-020-01430-1

11. Akcimen F, Spiegelman D, Dionne-Laporte A, Gan-Or Z, Dion PA, Rouleau GA. Screening of novel restless legs syndrome-associated genes in French-Canadian families. *Neurol-Genet*. Dec 2018;4(6)doi:ARTN e296
10.1212/NXG.0000000000000296
12. Schulte EC, Kousi M, Tan PL, et al. Targeted Resequencing and Systematic In Vivo Functional Testing Identifies Rare Variants in MEIS1 as Significant Contributors to Restless Legs Syndrome. *Am J Hum Genet*. Jul 13 2014;95(1):85-95. doi:10.1016/j.ajhg.2014.06.005
13. Tilch E, Schormair B, Zhao C, et al. Identification of Restless Legs Syndrome Genes by Mutational Load Analysis. *Ann Neurol*. Feb 2020;87(2):184-193. doi:10.1002/ana.25658
14. All of Us Research Program I, Denny JC, Rutter JL, et al. The "All of Us" Research Program. *N Engl J Med*. Aug 15 2019;381(7):668-676. doi:10.1056/NEJMSr1809937
15. Harrison SM, Austin-Tse CA, Kim S, et al. Harmonizing variant classification for return of results in the All of Us Research Program. *Hum Mutat*. Aug 2022;43(8):1114-1121. doi:10.1002/humu.24317
16. Venner E, Muzny D, Smith JD, et al. Whole-genome sequencing as an investigational device for return of hereditary disease risk and pharmacogenomic results as part of the All of Us Research Program. *Genome Med*. Mar 28 2022;14(1):34. doi:10.1186/s13073-022-01031-z
17. How the All of Us Genomic data are organized. 2023. <https://support.researchallofus.org/hc/en-us/articles/4614687617556-How-the-All-of-Us-Genomic-data-are-organized>
18. Awadalla P, Boileau C, Payette Y, et al. Cohort profile of the CARTaGENE study: Quebec's population-based biobank for public health and personalized genomics. *Int J Epidemiol*. Oct 2013;42(5):1285-99. doi:10.1093/ije/dys160
19. Forgetta V, Li R, Darmond-Zwaig C, et al. Cohort profile: genomic data for 26 622 individuals from the Canadian Longitudinal Study on Aging (CLSA). *BMJ Open*. Mar 10 2022;12(3):e059021. doi:10.1136/bmjopen-2021-059021
20. Manichaikul A, Mychaleckyj JC, Rich SS, Daly K, Sale M, Chen WM. Robust relationship inference in genome-wide association studies. *Bioinformatics*. Nov 15 2010;26(22):2867-73. doi:10.1093/bioinformatics/btq559
21. Manichaikul A, Mychaleckyj JC, Rich SS, Daly K, Sale M, Chen WM. Robust relationship inference in genome-wide association studies. *Bioinformatics*. Nov 2010;26(22):2867-2873. doi:10.1093/bioinformatics/btq559
22. Chang CC, Chow CC, Tellier LCAM, Vattikuti S, Purcell SM, Lee JJ. Second-generation PLINK: rising to the challenge of larger and richer datasets. *Gigascience*. Feb 25 2015;4doi:ARTN 7
10.1186/s13742-015-0047-8
23. Taliun D, Harris DN, Kessler MD, et al. Sequencing of 53,831 diverse genomes from the NHLBI TOPMed Program. *Nature*. Feb 11 2021;590(7845)doi:10.1038/s41586-021-03205-y
24. Fuchsberger C, Abecasis GR, Hinds DA. minimac2: faster genotype imputation. *Bioinformatics*. Mar 1 2015;31(5):782-784. doi:10.1093/bioinformatics/btu704
25. Das S, Forer L, Schonherr S, et al. Next-generation genotype imputation service and methods. *Nat Genet*. Oct 2016;48(10):1284-1287. doi:10.1038/ng.3656
26. Venables WN, Ripley BD. *Modern Applied Statistics with S. Fourth Edition*. 2002.
27. Willer CJ, Li Y, Abecasis GR. METAL: fast and efficient meta-analysis of genomewide association scans. *Bioinformatics*. Sep 1 2010;26(17):2190-1. doi:10.1093/bioinformatics/btq340
28. Murphy AE, Schilder BM, Skene NG. MungeSumstats: a Bioconductor package for the standardization and quality control of many GWAS summary statistics. *Bioinformatics*. Dec 7 2021;37(23):4593-4596. doi:10.1093/bioinformatics/btab665

29. Watanabe K, Taskesen E, van Bochoven A, Posthuma D. Functional mapping and annotation of genetic associations with FUMA. *Nat Commun*. Nov 28 2017;8doi:ARTN 1826
10.1038/s41467-017-01261-5
30. de Leeuw CA, Mooij JM, Heskes T, Posthuma D. MAGMA: Generalized Gene-Set Analysis of GWAS Data. *Plos Comput Biol*. Apr 2015;11(4)doi:ARTN e1004219
10.1371/journal.pcbi.1004219
31. McLaren W, Gil L, Hunt SE, et al. The Ensembl Variant Effect Predictor. *Genome Biol*. Jun 6 2016;17(1):122. doi:10.1186/s13059-016-0974-4
32. Karczewski KJ, Francioli LC, Tiao G, et al. The mutational constraint spectrum quantified from variation in 141,456 humans. *Nature*. May 2020;581(7809):434-443. doi:10.1038/s41586-020-2308-7
33. Gusev A, Ko A, Shi H, et al. Integrative approaches for large-scale transcriptome-wide association studies. *Nat Genet*. Mar 2016;48(3):245-52. doi:10.1038/ng.3506
34. Gamazon ER, Wheeler HE, Shah KP, et al. A gene-based association method for mapping traits using reference transcriptome data. *Nat Genet*. Sep 2015;47(9):1091-8. doi:10.1038/ng.3367
35. Mancuso N, Freund MK, Johnson R, et al. Probabilistic fine-mapping of transcriptome-wide association studies. *Nat Genet*. Apr 2019;51(4):675-682. doi:10.1038/s41588-019-0367-1
36. Casella AM, Colantuoni C, Ament SA. Identifying enhancer properties associated with genetic risk for complex traits using regulome-wide association studies. *Plos Comput Biol*. Sep 2022;18(9):e1010430. doi:10.1371/journal.pcbi.1010430
37. Kuleshov MV, Jones MR, Rouillard AD, et al. Enrichr: a comprehensive gene set enrichment analysis web server 2016 update. *Nucleic Acids Res*. Jul 8 2016;44(W1):W90-7.
doi:10.1093/nar/gkw377
38. Chen EY, Tan CM, Kou Y, et al. Enrichr: interactive and collaborative HTML5 gene list enrichment analysis tool. *BMC Bioinformatics*. Apr 15 2013;14:128. doi:10.1186/1471-2105-14-128
39. Bellenguez C, Kucukali F, Jansen IE, et al. New insights into the genetic etiology of Alzheimer's disease and related dementias. *Nat Genet*. Apr 2022;54(4):412-436. doi:10.1038/s41588-022-01024-z
40. Demontis D, Walters GB, Athanasiadis G, et al. Genome-wide analyses of ADHD identify 27 risk loci, refine the genetic architecture and implicate several cognitive domains. *Nat Genet*. Feb 2023;55(2):198-208. doi:10.1038/s41588-022-01285-8
41. Howard DM, Adams MJ, Clarke TK, et al. Genome-wide meta-analysis of depression identifies 102 independent variants and highlights the importance of the prefrontal brain regions. *Nat Neurosci*. Mar 2019;22(3):343-352. doi:10.1038/s41593-018-0326-7
42. Watanabe K, Jansen PR, Savage JE, et al. Genome-wide meta-analysis of insomnia prioritizes genes associated with metabolic and psychiatric pathways. *Nat Genet*. Aug 2022;54(8):1125-1132.
doi:10.1038/s41588-022-01124-w
43. Savage JE, Jansen PR, Stringer S, et al. Genome-wide association meta-analysis in 269,867 individuals identifies new genetic and functional links to intelligence. *Nat Genet*. Jul 2018;50(7):912-919. doi:10.1038/s41588-018-0152-6
44. Nagel M, Jansen PR, Stringer S, et al. Meta-analysis of genome-wide association studies for neuroticism in 449,484 individuals identifies novel genetic loci and pathways. *Nat Genet*. Jul 2018;50(7):920-927. doi:10.1038/s41588-018-0151-7
45. Bell S, Rigas AS, Magnusson MK, et al. A genome-wide meta-analysis yields 46 new loci associating with biomarkers of iron homeostasis. *Commun Biol*. Feb 3 2021;4(1):156.
doi:10.1038/s42003-020-01575-z

46. Bulik-Sullivan BK, Loh PR, Finucane HK, et al. LD Score regression distinguishes confounding from polygenicity in genome-wide association studies. *Nat Genet.* Mar 2015;47(3):291-5. doi:10.1038/ng.3211
47. Raina P, Wolfson C, Kirkland S, et al. Cohort Profile: The Canadian Longitudinal Study on Aging (CLSA). *Int J Epidemiol.* Dec 1 2019;48(6):1752-1753j. doi:10.1093/ije/dyz173
48. Nalls MA, Blauwendraat C, Vallerga CL, et al. Identification of novel risk loci, causal insights, and heritable risk for Parkinson's disease: a meta-analysis of genome-wide association studies. *Lancet Neurol.* Dec 2019;18(12):1091-1102. doi:10.1016/S1474-4422(19)30320-5
49. Mohtashami S, He Q, Ruskey JA, et al. TOX3 Variants Are Involved in Restless Legs Syndrome and Parkinson's Disease with Opposite Effects. *J Mol Neurosci.* Mar 2018;64(3):341-345. doi:10.1007/s12031-018-1031-4
50. Winkelmann J, Schormair B, Lichtner P, et al. Genome-wide association study of restless legs syndrome identifies common variants in three genomic regions. *Nat Genet.* Aug 2007;39(8):1000-1006. doi:10.1038/ng2099
51. Winkelmann J, Czamara D, Schormair B, et al. Genome-Wide Association Study Identifies Novel Restless Legs Syndrome Susceptibility Loci on 2p14 and 16q12.1. *Plos Genet.* Jul 2011;7(7)doi:ARTN e1002171 10.1371/journal.pgen.1002171
52. Akcimen F, Sarayloo F, Liao C, et al. Transcriptome-wide association study for restless legs syndrome identifies new susceptibility genes. *Commun Biol.* Jul 10 2020;3(1):373. doi:10.1038/s42003-020-1105-z
53. Xiong L, Catoire H, Dion P, et al. MEIS1 intronic risk haplotype associated with restless legs syndrome affects its mRNA and protein expression levels. *Hum Mol Genet.* Mar 15 2009;18(6):1065-1074. doi:10.1093/hmg/ddn443
54. Catoire H, Sarayloo F, Mourabit Amari K, et al. A direct interaction between two Restless Legs Syndrome predisposing genes: MEIS1 and SKOR1. *Sci Rep.* Aug 15 2018;8(1):12173. doi:10.1038/s41598-018-30665-6
55. Yan CH, Levesque M, Claxton S, Johnson RL, Ang SL. Lmx1a and lmx1b function cooperatively to regulate proliferation, specification, and differentiation of midbrain dopaminergic progenitors. *J Neurosci.* Aug 31 2011;31(35):12413-25. doi:10.1523/JNEUROSCI.1077-11.2011
56. Doucet-Beaupre H, Ang SL, Levesque M. Cell fate determination, neuronal maintenance and disease state: The emerging role of transcription factors Lmx1a and Lmx1b. *FEBS Lett.* Dec 21 2015;589(24 Pt A):3727-38. doi:10.1016/j.febslet.2015.10.020
57. Laguna A, Schintu N, Nobre A, et al. Dopaminergic control of autophagic-lysosomal function implicates Lmx1b in Parkinson's disease. *Nat Neurosci.* Jun 2015;18(6):826-35. doi:10.1038/nn.4004
58. Tilch E, Schormair B, Zhao C, et al. Identification of Restless Legs Syndrome Genes by Mutational Load Analysis. *Ann Neurol.* Feb 2020;87(2):184-193. doi:10.1002/ana.25658
59. Gan-Or Z, Zhou S, Ambalavanan A, et al. Analysis of functional GLO1 variants in the BTBD9 locus and restless legs syndrome. *Sleep Med.* Sep 2015;16(9):1151-5. doi:10.1016/j.sleep.2015.06.002
60. Distler MG, Palmer AA. Role of Glyoxalase 1 (Glo1) and methylglyoxal (MG) in behavior: recent advances and mechanistic insights. *Front Genet.* 2012;3:250. doi:10.3389/fgene.2012.00250
61. Stratmann B, Engelbrecht B, Espelage BC, et al. Glyoxalase 1-knockdown in human aortic endothelial cells - effect on the proteome and endothelial function estimates. *Sci Rep.* Nov 29 2016;6:37737. doi:10.1038/srep37737

62. Hara T, Toyoshima M, Hisano Y, et al. Glyoxalase I disruption and external carbonyl stress impair mitochondrial function in human induced pluripotent stem cells and derived neurons. *Transl Psychiatry*. May 8 2021;11(1):275. doi:10.1038/s41398-021-01392-w
63. Chegao A, Guarda M, Alexandre BM, et al. Glycation modulates glutamatergic signaling and exacerbates Parkinson's disease-like phenotypes. *NPJ Parkinsons Dis*. Apr 25 2022;8(1):51. doi:10.1038/s41531-022-00314-x
64. Angeloni C, Zambonin L, Hrelia S. Role of methylglyoxal in Alzheimer's disease. *Biomed Res Int*. 2014;2014:238485. doi:10.1155/2014/238485
65. Tomioka NH, Yasuda H, Miyamoto H, et al. Elfn1 recruits presynaptic mGluR7 in trans and its loss results in seizures. *Nat Commun*. Jul 22 2014;5:4501. doi:10.1038/ncomms5501
66. Matsunaga H, Aruga J. Trans-Synaptic Regulation of Metabotropic Glutamate Receptors by Elfn Proteins in Health and Disease. *Front Neural Circuits*. 2021;15:634875. doi:10.3389/fncir.2021.634875
67. Rasheed M, Khan V, Harripaul R, et al. Exome sequencing identifies novel and known mutations in families with intellectual disability. *BMC Med Genomics*. Aug 27 2021;14(1):211. doi:10.1186/s12920-021-01066-y
68. Dursun A, Yalnizoglu D, Yilmaz DY, et al. Biallelic mutations in ELFN1 gene associated with developmental and epileptic encephalopathy and joint laxity. *Eur J Med Genet*. Nov 2021;64(11):104340. doi:10.1016/j.ejmg.2021.104340
69. Sylwestrak EL, Ghosh A. Elfn1 regulates target-specific release probability at CA1-interneuron synapses. *Science*. Oct 26 2012;338(6106):536-40. doi:10.1126/science.1222482
70. Niswender CM, Conn PJ. Metabotropic glutamate receptors: physiology, pharmacology, and disease. *Annu Rev Pharmacol Toxicol*. 2010;50:295-322. doi:10.1146/annurev.pharmtox.011008.145533
71. Dunn HA, Patil DN, Cao Y, Orlandi C, Martemyanov KA. Synaptic adhesion protein ELFN1 is a selective allosteric modulator of group III metabotropic glutamate receptors in trans. *Proc Natl Acad Sci U S A*. May 8 2018;115(19):5022-5027. doi:10.1073/pnas.1722498115
72. Gasparini F, Di Paolo T, Gomez-Mancilla B. Metabotropic glutamate receptors for Parkinson's disease therapy. *Parkinsons Dis*. 2013;2013:196028. doi:10.1155/2013/196028
73. Consortium GT, Laboratory DA, Coordinating Center -Analysis Working G, et al. Genetic effects on gene expression across human tissues. *Nature*. Oct 11 2017;550(7675):204-213. doi:10.1038/nature24277
74. Vosa U, Claringbould A, Westra HJ, et al. Large-scale cis- and trans-eQTL analyses identify thousands of genetic loci and polygenic scores that regulate blood gene expression. *Nat Genet*. Sep 2021;53(9):1300-1310. doi:10.1038/s41588-021-00913-z

Table 1. Genome-wide association study results. *P*-values and the odds ratios were identified through a meta-analysis of the summary statistics (9,851 RLS cases and 38,957 controls). The variant with the lowest *p*-value is listed for each of the nine loci. The Bonferroni threshold for genome-wide significance was defined as 5.0×10^{-8} . Genes that are in close proximity to the top variants or identified by post-GWAS analyses are listed. Chr, chromosome; EA, effect allele; OA, other allele; *novel GWAS variant; †prioritized by TWAS or fine mapping.

Discovery meta-analysis					Follow up analysis (Didriksen et al.)		Joint stage meta-analysis	
Chr:position (hg38)	Alleles (OA, EA)	Gene(s)	OR (95% CI)	<i>p</i> -value	OR (95% CI)	<i>p</i> -value	OR (95% CI)	<i>p</i> -value
1:106,650,227	G, A	<i>PRMT6</i> †	1.12 (1.08–1.15)	1.50×10^{-11}	1.15 (1.11–1.18)	1.90×10^{-17}	1.13 (1.11–1.16)	3.14×10^{-27}
2:66,523,432	G, T	<i>MEIS1</i> †	1.66 (1.56–1.76)	2.36×10^{-56}	1.89 (1.89–2.00)	4.50×10^{-100}	1.77 (1.70–1.85)	4.50×10^{-152}
6:38,476,264	A, G	<i>BTBD9, GLO1</i> †	0.81 (0.78–0.84)	2.11×10^{-31}	0.77 (0.74–0.80)	1.55×10^{-50}	0.77 (0.79–0.81)	2.02×10^{-79}
7:1,340,813	C, G	<i>UNCX, ELFN1</i> †	0.90 (0.87–0.93)	2.16×10^{-9}	0.90 (0.87–0.93)	9.50×10^{-10}	0.90 (0.88–0.92)	1.17×10^{-17}
7:88,682,938	A, G	<i>ZNF804B, STEAP2</i> †	1.15 (1.10–1.21)	3.13×10^{-9}	1.13 (1.08–1.18)	1.69×10^{-7}	1.14 (1.10–1.18)	3.20×10^{-15}
9:8,822,069	G, A	<i>PTPRD, PTPRD-ASI</i> †	0.91 (0.88–0.94)	3.36×10^{-8}	0.92 (0.89–0.95)	9.05×10^{-8}	0.92 (0.90–0.94)	1.60×10^{-14}
9:126,755,162*	C, A	<i>LMX1B</i>	1.14 (1.09–1.19)	2.20×10^{-9}	1.10 (1.05–1.14)	2.60×10^{-5}	1.12 (1.08–1.15)	6.41×10^{-13}
15:67,816,234	C, T	<i>SKOR1</i> †, <i>MAP2K5</i> †	0.86 (0.83–0.89)	1.04×10^{-16}	0.83 (0.80–0.86)	2.02×10^{-28}	0.84 (0.82–0.87)	8.73×10^{-43}
16:52,610,538	A, C	<i>TOX3</i>	0.86 (0.83–0.89)	1.18×10^{-19}	0.82 (0.80–0.85)	5.88×10^{-34}	0.84 (0.82–0.86)	4.41×10^{-51}

Table 2. Gene-based association test results. Genome-wide gene-based test was done using MAGMA based on the meta-analysis of GWAS discovery cohorts (9,851 RLS cases and 38,957 controls). Bonferroni threshold for genome-wide significance was defined as 2.69×10^{-6} . The chromosomal position is shown according to hg38.

Chr	Start	Stop	Gene	p-value
2	66,660,584	66,801,001	<i>MEIS1</i>	1.27×10^{-12}
6	38,136,227	38,607,924	<i>BTBD9</i>	3.79×10^{-17}
6	38,643,701	38,670,917	<i>GLO1</i>	8.45×10^{-7}
15	68,112,042	68,126,899	<i>SKOR1</i>	6.37×10^{-12}
15	67,835,047	68,099,461	<i>MAP2K5</i>	3.84×10^{-10}
16	52,471,917	52,581,714	<i>TOX3</i>	5.77×10^{-13}

Table 3. Transcriptome-wide association study results. TWAS was performed using FUSION and S-PrediXcan based on the meta-analysis of GWAS discovery cohorts (9,851 RLS cases and 38,957 controls). Bonferroni correction threshold was defined as 2.10×10^{-6} for FUSION and 3.06×10^{-6} for S-PrediXcan. The chromosomal positions are shown according to hg38.

Tissue	Gene	Chr	Start	End	Model	TWAS Z-score	TWAS <i>p</i> -value	Software
cortex	<i>MEIS1</i>	2	66,433,452	66,573,869	elastic net	4.67	3.05×10^{-6}	S-PrediXcan
caudate (basal ganglia)	<i>GLO1</i>	6	38,703,140	38,703,141	susie	-5.51	3.68×10^{-8}	FUSION
cerebellar hemisphere	<i>GLO1</i>	6	38,703,140	38,703,141	lasso	-5.15	2.64×10^{-7}	FUSION
anterior cingulate cortex	<i>GLO1</i>	6	38,703,140	38,703,141	mashr	-5.54	3.01×10^{-8}	S-PrediXcan
caudate (basal ganglia)	<i>GLO1</i>	6	38,703,140	38,703,141	mashr	-4.84	1.28×10^{-6}	S-PrediXcan
caudate (basal ganglia)	<i>GLO1</i>	6	38,703,140	38,703,141	elastic net	-4.81	1.49×10^{-6}	S-PrediXcan
cerebellar hemisphere	<i>GLO1</i>	6	38,703,140	38,703,141	elastic net	-5.33	9.97×10^{-8}	S-PrediXcan
hippocampus	<i>GLO1</i>	6	38,703,140	38,703,141	mashr	-5.40	6.75×10^{-8}	S-PrediXcan
hypothalamus	<i>GLO1</i>	6	38,703,140	38,703,141	mashr	-5.39	6.94×10^{-8}	S-PrediXcan
nucleus accumbens	<i>GLO1</i>	6	38,703,140	38,703,141	elastic net	-5.50	3.76×10^{-8}	S-PrediXcan
nucleus accumbens	<i>GLO1</i>	6	38,703,140	38,703,141	mashr	-5.40	6.59×10^{-8}	S-PrediXcan
pituitary	<i>GLO1</i>	6	38,703,140	38,703,141	elastic net	-4.69	2.69×10^{-6}	S-PrediXcan
putamen (basal ganglia)	<i>GLO1</i>	6	38,703,140	38,703,141	elastic net	-4.67	2.97×10^{-6}	S-PrediXcan
substantia nigra	<i>GLO1</i>	6	38,703,140	38,703,141	mashr	-5.31	1.10×10^{-7}	S-PrediXcan
hippocampus	<i>ELFN1</i>	7	1,688,118	1,688,119	lasso	5.01	5.55×10^{-7}	FUSION
spinal cord	<i>UBASH3B</i>	11	122,655,675	122,814,473	mashr	-4.75	2.07×10^{-6}	S-PrediXcan
anterior cingulate cortex	<i>MAP2K5</i>	15	67,542,708	67,542,709	lasso	-5.99	2.12×10^{-9}	FUSION
amygdala	<i>SKOR1</i>	15	67,819,703	67,819,704	lasso	6.03	1.62×10^{-9}	FUSION
frontal cortex	<i>SKOR1</i>	15	67,819,703	67,819,704	lasso	5.68	1.37×10^{-8}	FUSION
hippocampus	<i>SKOR1</i>	15	67,819,703	67,819,704	mashr	6.29	3.17×10^{-10}	S-PrediXcan
putamen (basal ganglia)	<i>CAPNS1</i>	19	36,139,574	36,139,575	susie	-5.69	1.27×10^{-8}	FUSION

Table 4. Regulome-wide association study. RWAS was performed using MAGMA based on the meta-analysis of GWAS discovery cohorts (9,851 RLS cases and 38,957 controls). The chromosomal positions are shown according to hg38.

Tissue	Chr	Start	Stop	Z	p-value	Gene
Brain dorsotemporal prefrontal cortex	2	66536368	66537368	7.76	4.11×10^{-15}	<i>MEIS1</i>
Brain inferior temporal lobe	6	38374324	38375324	8.74	1.13×10^{-18}	<i>BTBD9</i>
Brain hippocampus middle	6	38701324	38702324	5.40	3.40×10^{-8}	<i>GLO1</i>
Brain angular gyrus	9	8820900	8821900	5.06	2.05×10^{-7}	<i>PTPRD</i>
Brain substantia nigra	15	67802662	67803662	8.19	1.28×10^{-16}	<i>MAP2K5</i>
Brain anterior caudate	16	52592188	52593188	8.91	2.66×10^{-19}	<i>CASC16</i>
Brain germinal matrix	16	52524888	52525888	5.48	2.15×10^{-8}	<i>TOX3</i>

Table 5. Genetic correlation analysis. The genome-wide genetic correlation was calculated using the LD score regression. r_G refers to the genetic correlation between two traits, and SE is the standard error of the genetic correlation. Bonferroni correction threshold was defined as 0.00625 ($\alpha = 0.05/8$).

Trait	r_G	SE	p-value
Neuroticism	0.40	0.08	5.4×10^{-7}
Depression	0.35	0.06	2.17×10^{-8}
Intelligence	-0.20	0.006	4.0×10^{-4}
Alzheimer's disease	-0.13	0.1	0.18
Serum iron	-0.09	0.07	0.20
Serum ferritin	-0.04	0.05	0.37
Insomnia	0.03	0.04	0.55
Attention deficit hyperactivity disorder	0.03	0.05	0.56

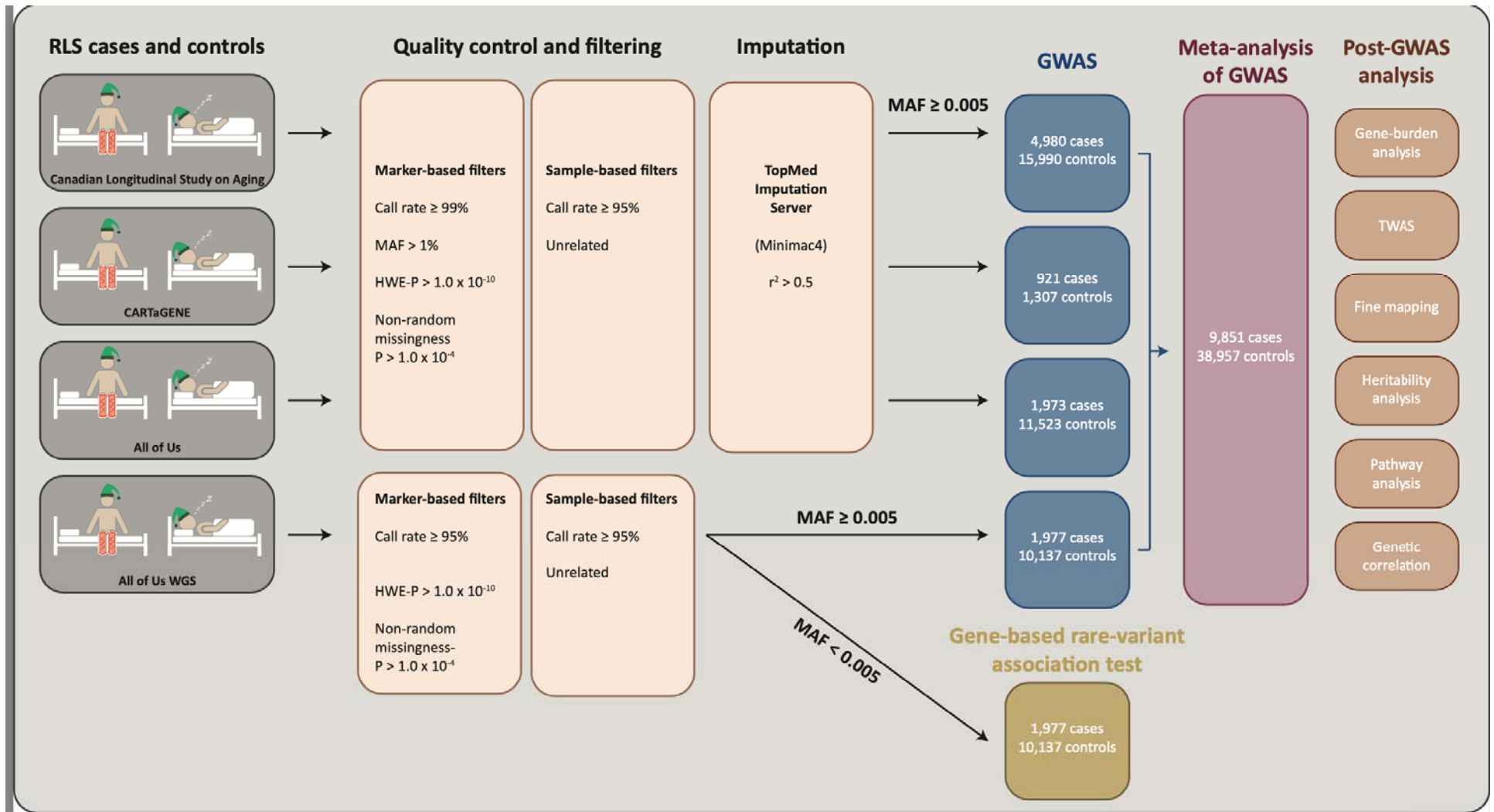


Figure 1. Workflow of the study.

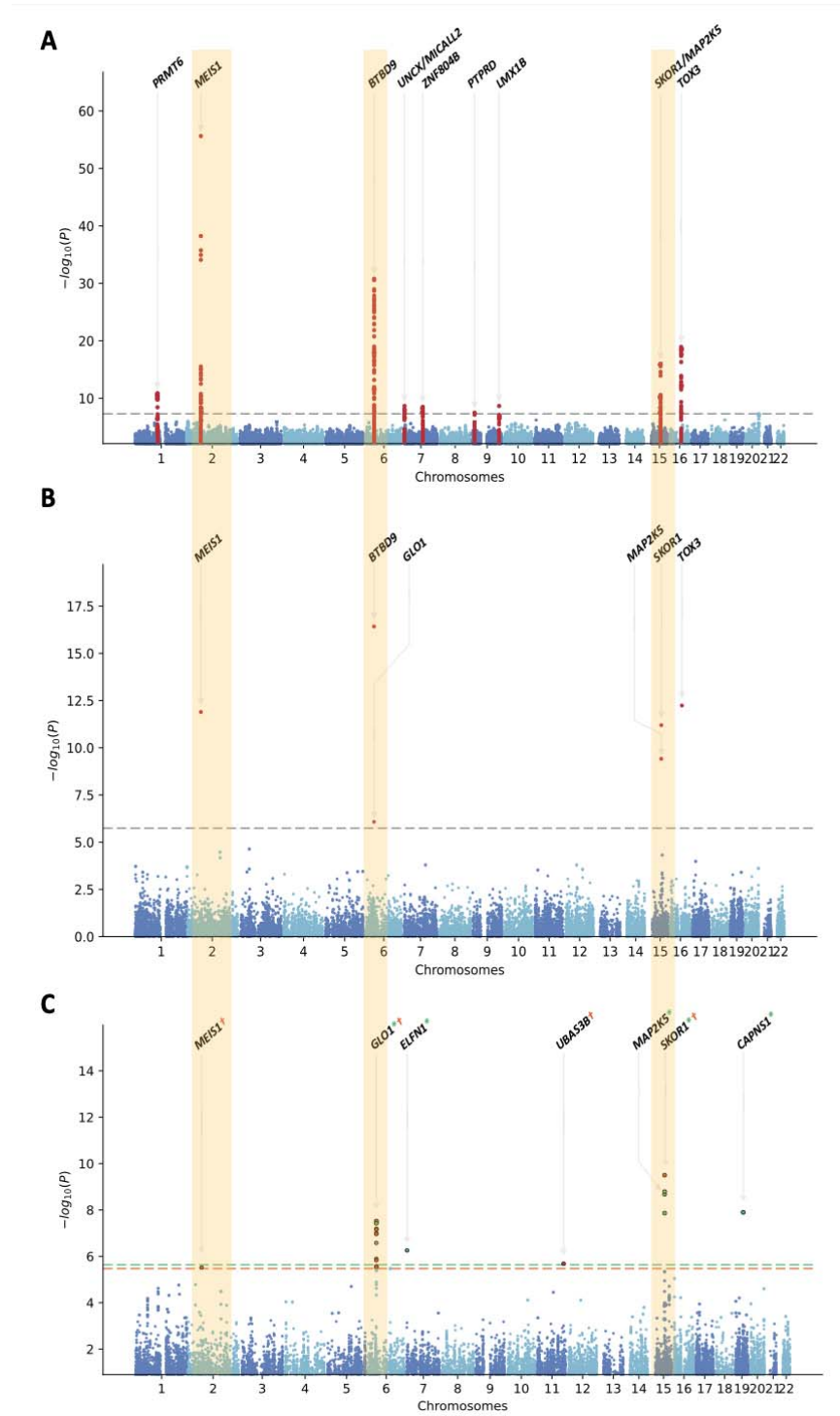


Figure 2. a. Manhattan plot for the RLS GWAS discovery cohort ($n = 9,851$ cases and $38,957$ controls; $\lambda_{1000} = 1.004$), **b.** gene-based common variant analysis using MAGMA (Bonferroni correction threshold = 2.69×10^{-6}), and **c.** gene-based transcriptome-wide association study results. Bonferroni threshold was set as 2.10×10^{-6} for FUSION and 3.06×10^{-6} for S-PrediXcan. Significant genes were labeled green (FUSION) and orange (S-PrediXcan).

Supplementary information

Supplementary Table 1. Demographic characteristics of study samples in GWAS discovery cohort. Diagnostic questions[†] in surveys and the Personal Medical History* domain were used to identify cases.

Dataset	Cases (% females)	Controls (% females)	Mean age, cases/controls	Population	RLS identifier questions
All of Us WGS*	1,977 (74%)	10,137 (75%)	62 (± 14), 62 (± 15)	United States	Has a doctor or health care provider ever told you that you have or had any of the following brain and nervous system conditions? (Restless legs syndrome)
All of Us GDA*	1,973 (73%)	11,523 (70%)	62 (± 14), 62 (± 15)		
CARTaGENE [†]	921 (67%)	13,07 (60%)	56 (± 8), 56 (± 8)	Quebec (Canada)	Do you have restless legs syndrome?
					Generally, your discomforts are worse...at rest/during activity/no difference/prefer not to answer/do not know
					Generally, your discomforts are relieved by... walking or movement/immobility or relaxation/prefer not to answer/do not know
					Generally, your discomforts are worse... in the morning/in the afternoon/evening, bedtime, night/no difference/prefer not to answer/do not know
Canadian Longitudinal Study on Aging [†]	4,980 (60%)	15,990 (47%)	63 (± 10), 63 (± 10)	Canada	Do you have, or have you sometimes experienced, a recurrent need or urge to move your legs while sitting or lying down?
Total number	9,851	38,957			

Supplementary Table 2. Gene mapping in the RLS risk regions. Annotation was performed in FUMA (v.1.5.1). It is provided as an Excel file.

Supplementary Table 3. Adjusted covariates in the logistic regression test. Covariates were selected using the MASS stepwise function. PC, principal component.

Dataset	List of the covariates
CARTaGENE	sex, age, PC1, PC2, PC4, PC7, PC10
Canadian Longitudinal Study on Aging	sex, age, PC2, PC6
All of Us	sex, age, PC3, PC8, PC9, PC10
All of Us WGS	sex, age, PC2, PC3, PC7, PC10

Supplementary Table 4. Replication of other known RLS risk variants in our meta-analysis.

Chr	Position (hg38)	EA/OA	Closest gene(s)	Direction	OR	P
2	3,986,856	G/A	<i>DCDC2C</i>	++++	1.08 (1.05–1.12)	3.03×10^{-6}
2	158,343,323	T/C	<i>CCDC148</i>	----	0.93 (0.90–0.97)	3.14×10^{-4}
2	189,584,800	T/A	<i>SLC40A1</i>	----	0.96 (0.93–0.99)	0.016
2	67,842,758	A/C	<i>C1D</i>	NA	NA	NA
3	3,406,460	T/A	<i>CRBN</i>	----	0.94 (0.90–0.97)	3.69×10^{-4}
3	130,816,723	G/A	<i>ATP2C1</i>	++++	1.07 (1.04–1.11)	6.25×10^{-5}
5	171,001,975	T/C	<i>RANBP17</i>	NA	NA	NA
6	37,522,755	G/A	<i>CCDC167</i>	++++	1.09 (1.05–1.14)	1.75×10^{-5}
9	9,290,311	T/C	<i>PTPRD, PTPRD-AS1</i>	----	0.95 (0.91–0.98)	1.76×10^{-3}
11	8,313,948	A/G	<i>LMO1</i>	NA	NA	NA
13	72,274,018	T/G	<i>DACH1</i>	++++	1.07 (1.03–1.11)	6.40×10^{-4}
15	47,068,169	T/G	<i>SEMA6D</i>	----	0.90 (0.85–0.95)	2.01×10^{-4}
15	35,916,797	T/A	<i>DPH6</i>	----	0.90 (0.84–0.96)	3.01×10^{-3}
17	48,695,414	A/G	<i>PRAC1</i>	++++	1.04 (1.00–1.08)	0.08
18	44,290,278	T/C	<i>SETBP1</i>	++++	1.05 (1.01–1.09)	0.01
18	59,943,413	T/C	<i>PMAIP1</i>	NA	NA	NA

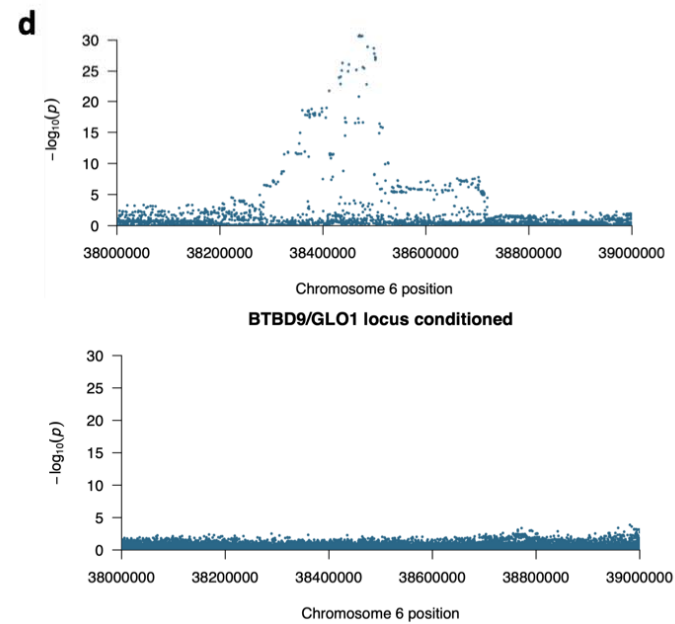
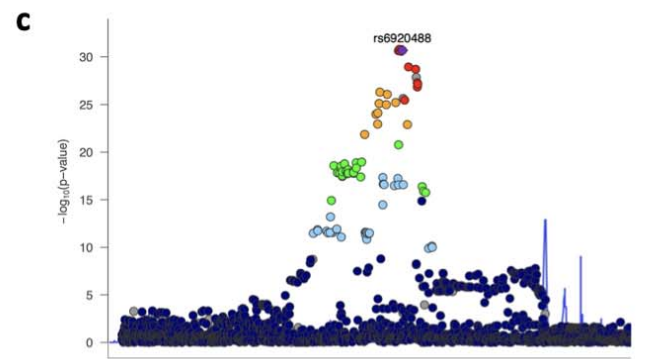
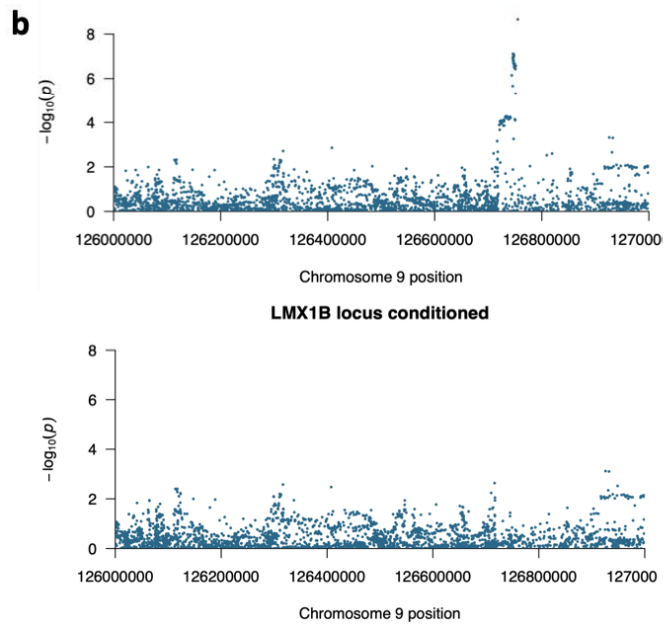
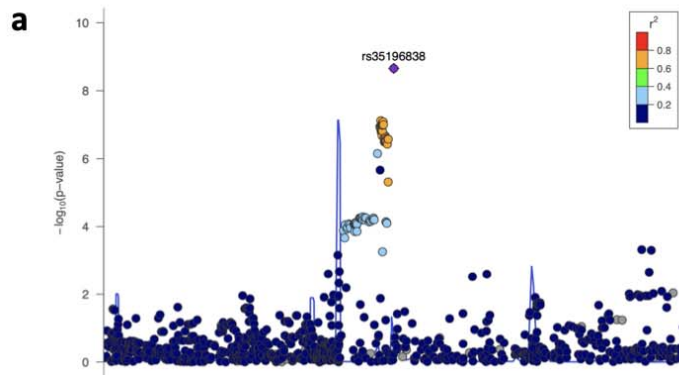
20 64,164,052 G/A *MYT1* ---- 0.91 (0.88–0.94) 1.17×10^{-7}

Supplementary Table 5. Causal posterior probabilities for genes in 90%-credible sets for restless legs syndrome transcriptome-wide association study signals. PIP, posterior inclusion probability.

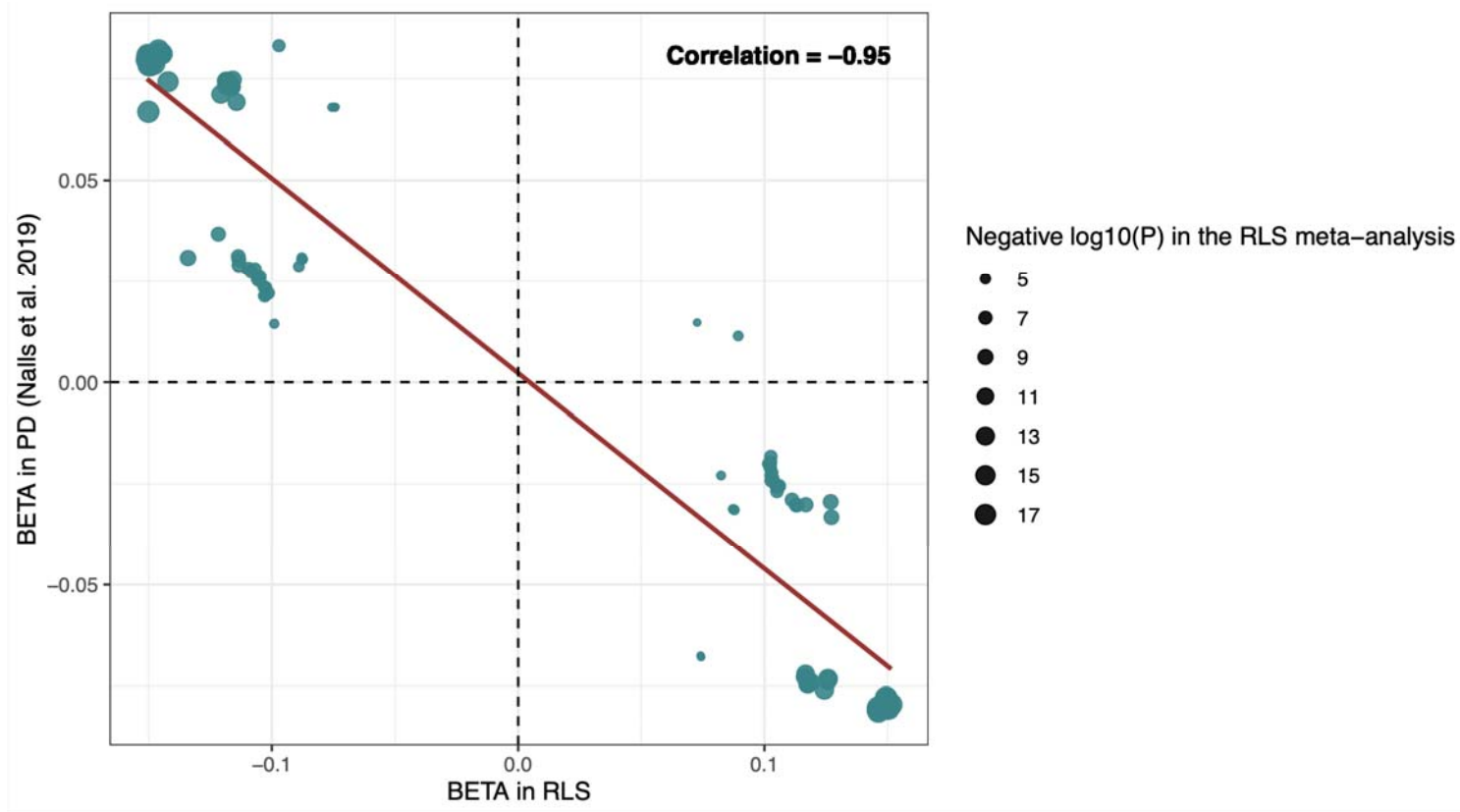
Gene	Region	Number of genes in the region	Proxy tissue	Method	PIP
<i>PRMT6</i>	1:105545220-107867043	16	spinal cord	lasso	0.06
<i>STEAP2</i>	7:88195689-91032469	35	spinal cord	susie	0.06
<i>GTPBP10</i>	7:88195689-91032469	35	nucleus accumbens	lasso	0.02
<i>PTPRD-AS1</i>	9:8456299-9166403	7	spinal cord	susie	0.13
<i>SKOR1</i>	15:66802429-68725660	30	nucleus accumbens	susie	0.69

Supplementary Table 6. Regulome-wide association study (RWAS) results. RWAS was done using MAGMA (v.1.06). Bonferroni correction threshold for each tissue was defined based on the number of enhancers tested. It is provided as an Excel file.

Supplementary Table 7. Gene sets and pathways identified by EnrichR using GO biological process and Reactome pathway datasets.

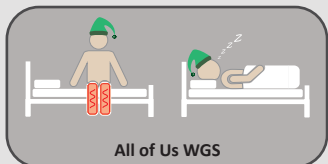
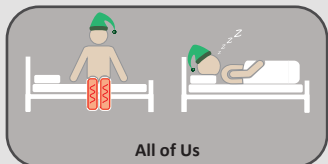
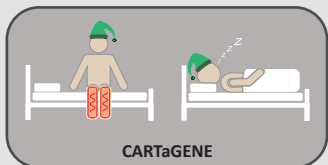
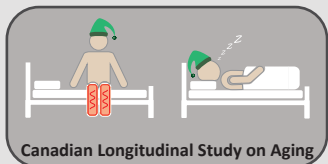


Supplementary Figure 1. a. LocusZoom plot for chr9:126755162:C:A, **b.** Conditional analysis at the *LMX1B* locus (before and after conditioning), **c.** LocusZoom plot for chr6:38476264:A:G, **d.** Conditional analysis at the *BTBD9/GLO1* locus (before and after conditioning).



Supplementary Figure 2. Beta-beta plot for *TOX3* variants in the RLS meta-analysis and Parkinson's disease meta-analysis. We compared the effect of the *TOX3* variants ($P < 1 \times 10^{-4}$) identified in our discovery meta-analysis with the recent Parkinson's disease GWAS by Nalls et al. [ref]. For the top significant variant in Parkinson's disease (16:52602330:C:A, hg38), we included the beta value from the meta-analysis, whereas, for the rest of the variants, we included summary statistics without 23andMe datasets. A negative correlation was found between the effects of *TOX3* variants in RLS and PD (The correlation coefficient is -0.95, and the Pearson correlation R^2 is 91).

RLS cases and controls



Quality control and filtering

Marker-based filters

Call rate $\geq 99\%$

MAF $> 1\%$

HWE-P $> 1.0 \times 10^{-10}$

Non-random missingness
P $> 1.0 \times 10^{-4}$

Sample-based filters

Call rate $\geq 95\%$

Unrelated

Marker-based filters

Call rate $\geq 95\%$

HWE-P $> 1.0 \times 10^{-10}$

Non-random missingness-
P $> 1.0 \times 10^{-4}$

Sample-based filters

Call rate $\geq 95\%$

Unrelated

Imputation

TopMed
Imputation
Server
(Minimac4)

$r^2 > 0.5$

GWAS

MAF ≥ 0.005

4,980 cases
15,990 controls

921 cases
1,307 controls

1,973 cases
11,523 controls

1,977 cases
10,137 controls

MAF ≥ 0.005

MAF < 0.005

Gene-based rare-variant
association test

1,977 cases
10,137 controls

Meta-analysis of GWAS

9,851 cases
38,957 controls

Post-GWAS analysis

Gene-burden
analysis

TWAS

Fine mapping

Heritability
analysis

Pathway
analysis

Genetic
correlation